INTERNATIONAL JOURNAL OF CIRCUITS, SYSTEMS AND SIGNAL PROCESSING
DOI: 10.46300/9106.2023.17.11 Volume 17, 2023

Spectral Efficiency Performance of Multi Cell MIMO Systems in Impulsive Noise Channels

H. Abu Hilal
Higher Colleges of Technology, UAE

Received: August 19, 2022. Revised: January 20, 2023. Accepted: February 22, 2023. Published: March 6, 2023.

Abstract: This research report details how impulsive noise affects communication systems. This research evaluates the differences and similarities among impulse models in communication systems. After comparing and contrasting the impulse noise models' similarities and differences, the models' service execution will be compared. Spectral efficiency is the fundamental criterion for comparing models' service execution. Comparing models under different impulse noise levels and inter- cell and intra-cell intercession will also be done. The 5G mm Wave multiple input/output system's service execution will be researched. The study will use IN. First, the Gaussian noise scenario will be deduced for the stated device's performance, followed by the non- Gaussian noise scenario derivation. The latter deriva- tion also involves averaging Gaussian noise in terms of impulsive noise's spread. Monte Carlo simulations are used to show and support derivations.

Keywords: MultiCell, Impulsive Noise, Massive MIMO, mmWave, 5G

I. INTRODUCTION

In terms of performance and security, 4G and 5G wireless connections must be adjusted. Average cell input, data ratio, energy and spectral efficiency (EE and SE) must be improved in the 5G network (Fig 1).A number of research projects have been launched to find the best options for adjusting the given parameters. Massive multiple-input massive-output technology is one of these studies' significant inventions (MIMO). This method adjusts network traffic and reliability by placing many antennas at base stations, ([1–4]). A faster 5G network would speed up service delivery and operations in the military, entertainment, health, and education sectors. For speedier communication, the radio spectrum must be more efficient and faster. This is crucial since 5G wireless communications rely on radio frequency. Other tools and qualities include strong culminating output and stubby dormancy. Spectral efficiency intensification must be a top concern while constructing an effective 5G network. A considerable portion of the 5G network's critical spectrum is stolen from earlier wireless networks. 5G network success requires advances in baseband radio frequency structures, radio frequency domain handling, and network design, structures, ([5–9]).

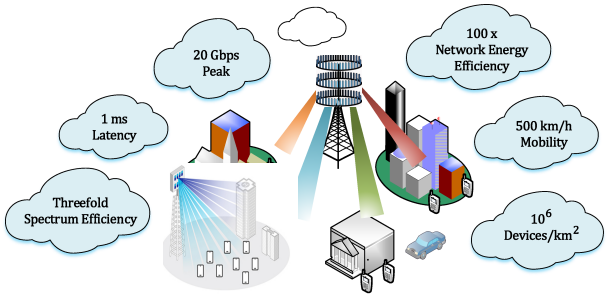

Fig. 1 General KPI's of the Massive MIMO system.

II. LITERATURE REVIEW

Many research have shown the availability of impulsive noise (IN) in different environmental ranges, but this venture has never received the priority it deserves during communication system evaluation. When a transceiver strategy is developed without Gaussian noise, service execution degrades. This performance decrease is prevalent in impulsive, intrusive settings. Just-released technology intended to improve 5G network dormancy, connection difficulties, and spectrum efficiency. It's been shown that impulsive networks can degrade service execution. NOMA technology is used. Spectral efficiency (SE) is vital to mobile communications, thus it's constantly improved. 5G networks must also prioritize spectral efficiency for accreditation. Validating 3 5G spectral efficiency modifications requires improvement. Novel multiple access technology uses sparse code for multiplexing, filtered orthogonal frequency distribution for waveform, and polar codes for channel coding. Multiple inputs and outputs (MIMO) systems are also examined for their dimensional modification strategy. An approach using order statistics and linear techniques is given for MIMO multicell multiuser systems. In the investigation, EE and SE are analyzed. Impulsive noise (IN) is utilized to evaluate NOMA's power domain so that IN issues can be understood and mitigated. In numerous communication systems practical applications, such as smart grid communications, IN is present, [12], [10] and [11].

Impulsive noise interferes with 5G network performance. Impulsive noise is harmful since ordinary receivers can't detect it. The two-state Markov-Gaussian process discusses the deterioration of service execution efficiency by object-oriented impulsive noise and approaches to ameliorate it. ([13–24]). Maximum a posteriori (MAP) receivers with sequential intercession repealing were suggested to reduce impulsive noise on users' detectors. The performance of 5G mm Wave under impulsive noise raises many research questions. When constructing a high-efficiency 5G network, spectral efficiency must be prioritized. More of the 5G network's critical spectrum is borrowed from previous wireless networks. This study's main accomplishment so far is examining spectral efficiency variables in impulsive noise conditions. Enhancing spectral efficiency under the Gaussian noise model for 5G network development is sometimes considered a normal problem. However, it is of great interest to find out if spectral efficiency is important in impulsive, Gaussian, and non-Gaussian noise models. We will examine non-Gaussian and Gaussian noise models to highlight spectral efficiency performance in the current model and lay a foundation for future work on 5G spectral efficiency in diverse noise models. This work aims to verify spectral simulations.

The paper is organized as follows: The multicell MIMO signals are presented in Section II, which explains the other signal components as well as calculating the signals and noise components for massive MIMO systems. Section III gives numerical evaluations and analysis. Conclusions are stated out in the last Section.

A. Notations

The transpose of a matrix $\mathbf{A}$ is symbolized by $\mathbf{A}^t$, and the Hermitian is indicated by $\mathbf{A}^H$. The bold case signifies matrix or vectors. The mathematical operator $\|\|$ is meaning the norm of the matrix. The $[\mathbf{A}]_k$ stances for the kth row of the matrix $\mathbf{A}$. $\mathbf{A}_{i,j}$ is the (i,j)th element of the matrix $\mathbf{A}$. The operation $E[x]$ is the expected value or the average of the random variable x. $*$ denotes for the complex conjugant.

III. SYSTEM MODEL

This section describes a multicell-based huge MIMO system. First, a general multicell system and impulsive noise type description is given. After the system explanation, we'll discuss simulation findings. Multicell systems let users connect to multiple cells at once. In this study, we'll examine a MIMO multicell with L cells and K users. Assume that the cell base station has more antennas than users ($M > K$). This analysis assumes mobile terminals have one antenna and the channel model has two portions. Path loss and shadowing effects are symbolised by β_{jk}, where β_{ljk} is the channel gain of the kth user from the jth to the lth cell. For the models second section, fading assumption is used to determine the channel gain coefficient from the j-th cell to the m-th antenna at the l-th cell by the kth user. In the equation above, $_U$ denotes the SNR, y_l is the complex vector of length M in the l-th base station.

$$\mathbf{y}_l = \sqrt{\rho_u} \sum_{i=1}^{L} \mathbf{G}_{l,i}\mathbf{x}_i + \mathbf{W}_l, \tag{1}$$

where $\mathbf{y}_l$ is the established complex vector of length M for the lth base station. ρ_u is the traditional SNR. $\mathbf{x}_i$ is a K dimensional vector, holding the transferred signals for the users in cell i. $\mathbf{G}_{l,i} = (g_{limk})_{M\times K}$, is a matrix that has a size of $M \times K$ and designates the channel elements between the lth base station and the K users in the ith cell. $l, i = 1, 2, ..., L$.

So that the (m,k)th element of (g_{limk}) is the channel figure between the mth antenna of the lth cell, and the kth user of the ith cell. Lastly, we can characterize (g_{limk}) as below:

$$g_{limk} = h_{limk}\sqrt{\beta_{lik}}, \tag{2}$$

$$\mathbf{G}_{li} = \mathbf{H}_{li}\beta_{li}, \qquad l, i = 1, 2, ..., L, \tag{3}$$

$$\beta_{li} = diag(\sqrt{\beta_{li1}}, \sqrt{\beta_{li2}}, ..., \sqrt{\beta_{liK}}), \tag{4}$$

where $\mathbf{H}_{l,i} = (h_{limk})_{M\times K}$. Finally, we describe the noise model in the system. In this research, we put forward the assumption that the noise term $\mathbf{W}_l$ is non Gaussian noise.

A. Impulsive Noise Model

For the impulsive noise model,the complex valued noise probability function is stated as follows:

$$p(w_p) = 2e^{-Z}\sum_{m=0}^{\infty}\frac{Z^m w_p e^{(-\frac{|w_p|^2}{2\sigma_m^2})}}{m!\sigma_m^2}, \tag{5}$$

where $\sigma_m^2 = (m/Z + X)/(X + 1)$, and $\sigma^2 = \text{var}(w_p)$. X characterizes the power relation of the background Gaussian noise and the impulsive one. Z is the impulsive index. It consequences in an impulsive w_i for minor values of Z, and a near-Gaussian when Z is large. Afterward we will set $\alpha_m = \frac{Z^m}{m!}exp(-Z)$ for ease. Consequently, w_p , when conditioned on a Poisson random variable Y_p with parameter Z, is Gaussian with zero mean and variance given by:

$$v_p = \text{var}(w_p/Y_p) = \sigma^2\left(\frac{Y_p}{Z(X+1)} + \frac{X}{X+1}\right), \tag{6}$$

We undertake $v_1 = v_2 = ...v_{N_R}$, and v is connected to a single poisson random variable P as in eq(6). This is true when the dissimilar diversity branches are subjectively influenced by the same physical process, making the conditional variance $v_p$of each division the same (independent of p). This could be a model for a multi-antenna system with close-packed antennas. Noise sample distribution $\mathbf{w} = [w_1, ..., w_M]$ is:

$$p(\mathbf{w}) = \sum_{m=0}^{\infty}\frac{\alpha_m}{(\pi\sigma_m^2)^M}e^{\left(-\sum_{p=1}^{M}\frac{|w_p|^2}{\sigma_m^2}\right)}, \tag{7}$$

Class A's noise model parameters are: Z is the overlap index, which is determined from the average number of impinging emission events per second and the average duration of each. X is the power ratio of the independent Gaussian portion and impulsive non-Gaussian element, in the range $[10^{-6}, 1]$.

This study addresses a two-cell network where each UE and BS have the same average channel gain. This tractable model has few parameters and was utilized in [26]. Consider cells 0 and 1. Uplink (UL). Cell 0 UEs broadcast to their serving BS, while cell 1 UEs leak into cell 0. The typical fading channel element from cell 0 UE to its assisting BS is β_0^0 while cell 1 UE intrusive signals haveβ_1^0.

The average fading channel element from a UE in cell 1 to its serving BS is β_1^1, while interfering waveforms from UEs in cell 0 have β_0^1.

Superscript denotes the receiving BS cell and subscript shows the sending user equipment cell. When calculating SE, interference strength is most important.

$$\widehat{\beta} = \frac{\beta_1^0}{\beta_0^0} = \frac{\beta_0^1}{\beta_0^0} = \frac{\beta_1^0}{\beta_1^1} = \frac{\beta_0^1}{\beta_1^1} \tag{8}$$

It is conjoint to have $0 < \widehat{\beta} < 1$ where $\widehat{\beta} \approx= 0$ stances for feeble inter cell interference, and $\widehat{\beta} \approx= 1$ means that the intercell inteference is as strong as the desired signal (cell edge scenario). The received Signal to Noise Ratio (SNR) can be written as SNR= $\frac{P}{\sigma^2}\beta_0^0$

P is the UE's transmitted power and $\sigma^2$is noise. We start with a single antenna, single user per cell approach to explain our technology. Assuming a flat fading channel, the symbol sampled complex baseband signal ($y_0 \in C$)at cell 0 BS is:

$$y_0 = h_0^0 s_0 + h_1^0 s_1 + n_0, \tag{9}$$

where the relations in eq(9) are the desired signal, interfering signal and noise sample, therefore. $h_i^0 \sim N_C(0, \beta_i^0)$ is the well known Rayleigh model with $E\{\|h_i^0\|^2\}$ $=\beta_i^0$ and $h_i^0 = \sqrt{\beta_i^0}$. When the BS in cell 0 knows the channel response of the system UE SE can be found for both line of sight (LOS) and none LON (NLOS) cases. To start the derivation easily. Consider simple input output system given by $y = hx + n$, assuming for now the noise $n \sim N_C(0, \sigma^2)$, the input distribution is power limited as $E\{|x|^2\} \leq P$. If h is deterministic then the channel capacity $C = \log_2(1 + \frac{p|h|^2}{\sigma^2})$ and achieved by the input distribution $X \sim N_C(0, \sigma_p^2)$, if H is a realization of a random variable H independent of the signal and noise then, $C = E\{\log_2(1 + \frac{P|h|^2}{\sigma^2}\}$, then we can write the UL SE LOS as (using the Identity (1) in the appendix):

$$\text{SE}_0^{\text{LOS}} = \log_2(1 + \frac{1}{\widehat{\beta} + \frac{1}{SNR_0}}), \tag{10}$$

and the NLOS with $\widehat{\beta} \neq 1$ the achievable UL SE is

$$\begin{aligned}\text{SE} &= E\{\log_2(1+\frac{P|h_0^0|^2}{P|h_1^0|^2+\sigma^2})\}\\ &= E\{\log_2(1+\sum_{i=0}^{1}\frac{P|h_i^0|^2}{|h_1^0|^2+\sigma^2})\}-E\{\log_2(1+\frac{P|h_1^0|^2}{\sigma^2})\}\\ &= E\{\log_2(1+\frac{P|h_0^0|^2}{P|h_1^0|^2+\sigma^2})\}\end{aligned}$$

$$\text{SE}_0^{\text{NLOS}} = \frac{e^{\frac{1}{\text{SNR}_0}}E_1(\frac{1}{\text{SNR}_0})-e^{\frac{1}{\text{SNR}_0\widehat{\beta}}}E_1(\frac{1}{\text{SNR}_0\widehat{\beta}})}{log_e(2)(1-\widehat{\beta})}, \quad (11)$$

where $E_1 = \int_1^\infty e^{-Xu}\frac{du}{u}$. Now, assuming the UE has an array of antennas and maximal ratio combining is adopted, we can the write the following vector equations (for SIMO):

$$\mathbf{y}_0 = \mathbf{h}_0^0 S_0 + \mathbf{h}_1^0 S_1 + \mathbf{n}_0, \quad (12)$$

$$\mathbf{h}_i^0 = \sqrt{\beta_i^0}\left[1\ e^{2\pi j d_H sin(\phi_i^0)}\ ...\ e^{2\pi j d_H(M-1)sin(\phi_i^0)}\right]^T, \quad (13)$$

where λ is the wavelength of the carrier frequency $\phi_i^0 \in [0\ 2\pi)$ is the azimuth angle to the UE. For MRC where we multiply the received vector in eq(13) by $\mathbf{v}_0 = \mathbf{h}_0^0$ hence this maximizes the ratio $\frac{|\mathbf{v}_0^H\mathbf{h}_0^0|^2}{\|\mathbf{v}_0\|^2}$. For LOS we can write:

$$\begin{aligned}\text{SE} &= \{\log_2(1+\frac{P\|\mathbf{h}_0^0\|^4}{P|(\mathbf{h}_0^0)^H\mathbf{h}_1^0|^2+\sigma^2\|\mathbf{h}_0\|^2})\}\\ &= \{\log_2(1+\frac{P\|\mathbf{h}_0^0\|^2}{\frac{P|(\mathbf{h}_0^0)^H\mathbf{h}_1^0|^2}{\|\mathbf{h}_0\|^2}+\sigma^2}),\\ \text{SE} &= \{\log_2(1+\frac{P\|\mathbf{h}_0^0\|^2}{\frac{P|(\mathbf{h}_0^0)^H\mathbf{h}_1^0|^2}{\|\mathbf{h}_0\|^2}+\sigma^2})\} \quad (14)\end{aligned}$$

where $\|\mathbf{h}_0\|^2 = \beta_0^0 M$ for M antenna system.

$$\begin{aligned}\mathbf{h}_0^0\mathbf{h}_1^0 &= \sqrt{\beta_0^0\beta_1^0}\sum_{m=0}^{M-1}\left(e^{j2\pi d_H(sin\phi_1^0-sin\phi_0^0)}\right)^m\\ &= \sqrt{\beta_0^0\beta_1^0}M\ \ ,\ \ (sin\phi_1^0 = sin\phi_0^0)\ ,\\ &= \sqrt{\beta_0^0\beta_1^0}\frac{1-e^{2\pi j d_H M(sin\phi_1^0-sin\phi_0^0))}}{1-e^{2\pi j d_H(sin\phi_1^0-sin\phi_0^0))}}\ ,(sin\phi_1^0 \neq sin\phi_0^0)\end{aligned} \quad (15)$$

Utilizing the geometrical series formula $\sum_{m=0}^{M-1}x^m = \frac{1-x^M}{1-x}$ for $x \neq 1$, and $\sum_{m=0}^{M-1}x^m = M, x = 1$ and the below fact

$$\begin{aligned}&\left|\frac{1-e^{2\pi j d_H M(sin\phi_1^0-sin\phi_0^0))}}{1-e^{2\pi j d_H(sin\phi_1^0-sin\phi_0^0))}}\right|^2\\ &= \frac{sin^2(\pi d_H M(sin\phi_1^0-sin\phi_0^0))}{sin^2(\pi d_H(sin\phi_1^0-sin\phi_0^0))}\ ,\end{aligned}$$

$$\frac{|\mathbf{h}_0^0\mathbf{h}_1^0|^2}{\|\mathbf{h}_0^0\|^2} = \beta_1^0 g(\phi_0^0,\phi_1^0) \quad (16)$$

$$g(\phi,\psi) = \frac{sin^2(\pi d_H M(sin\phi-sin\psi))}{Msin^2(\pi d_H(sin\phi-sin\psi))}\ if\ (sin\phi \neq sin\psi) \quad (17)$$

$$g(\phi,\psi) = M\ if\ (sin\phi = sin\psi) \quad (18)$$

For the NLOS we can write the following equation:

$$\begin{aligned}\text{SE}^{\text{NLOS}} &= E_h\{\log_2(1+\frac{P\|\mathbf{h}_0^0\|^4}{P|(\mathbf{h}_0^0)^H\mathbf{h}_1^0|^2+\sigma^2\|\mathbf{h}_0\|^2})\}\\ &= E_h\{\log_2(1+\frac{P\|\mathbf{h}_0^0\|^2}{\frac{P|(\mathbf{h}_0^0)^H\mathbf{h}_1^0|^2}{\|\mathbf{h}_0\|^2}+\sigma^2})\}\\ &= E_h\{\log_2(1+\frac{P\|\mathbf{h}_0^0\|^2}{\sigma^2}+\frac{P}{\sigma^2}\left|\frac{(\mathbf{h}_0^0)^H\mathbf{h}_1^0}{\|\mathbf{h}_0^0\|}\right|^2)\}-\\ &E_h\{\log_2(1+\frac{P}{\sigma^2}\left|\frac{(\mathbf{h}_0^0)^H\mathbf{h}_1^0}{\|\mathbf{h}_0^0\|}\right|^2)\}\end{aligned} \quad (19)$$

where $\sqrt{\frac{P}{\sigma^2}}\frac{(\mathbf{h}_0^0)^H\mathbf{h}_1^0}{\|\mathbf{h}_0^0\|} \sim N_C(0,\text{SNR}_0\widehat{\beta})$. To find an expression for the second expected value term in eq(19), we use Identity (1) in the appendix. So:

$$E_h\{\log_2(1+\frac{P}{\sigma^2}\left|\frac{(\mathbf{h}_0^0)^H\mathbf{h}_1^0}{\|\mathbf{h}_0^0\|}\right|^2)\} = \frac{e^{\frac{1}{\text{SNR}_0\widehat{\beta}}}E(\frac{1}{\text{SNR}_0\widehat{\beta}})}{\log_2 e}, \quad (20)$$

Using Identity (1) in the appendix, wedetermine the first expected value word in eq(19):

$$E_h\{\log_2(1+\frac{P\|\mathbf{h}_0^0\|^2}{\sigma^2}+\frac{P}{\sigma^2}\left|\frac{(\mathbf{h}_0^0)^H\mathbf{h}_1^0}{\|\mathbf{h}_0^0\|}\right|^2)\}=$$
$$=\sum_{m=1}^{M}\sum_{l=0}^{M-m}\frac{(-1)^{M-L+1}}{(\frac{1}{\mathrm{SNR}_0\widehat{\beta}}-\frac{1}{\mathrm{SNR}_0})^m}\times$$
$$\left(\frac{e^{\frac{1}{\mathrm{SNR}_0}}E_1(\frac{1}{\mathrm{SNR}_0})+\sum_{n=1}^{L}\frac{1}{n}\sum_{j=0}^{n-1}\frac{1}{n!\mathrm{SNR}_0^j}}{(M-m-l)!\mathrm{SNR}_0^{M-l}\widehat{\beta}\log_e 2}\right)+$$
$$e^{1/\mathrm{SNR}_0}(\frac{1}{\mathrm{SNR}_0}-\frac{1}{\mathrm{SNR}_0\widehat{\beta}})^M\frac{E_1(1/\mathrm{SNR}_0)}{{\mathrm{SNR}_0}^M\log_e 2}$$
$$=\sum_{m=1}^{M}\sum_{l=0}^{M-m}\frac{(-1)^{M-m-L+1}}{(1-\frac{1}{\widehat{\beta}})^m}\times$$

$$\left(\frac{e^{\frac{1}{\mathrm{SNR}_0}}E_1(\frac{1}{\mathrm{SNR}_0})+\sum_{n=1}^{L}\frac{1}{n}\sum_{j=0}^{n-1}\frac{1}{n!\mathrm{SNR}_0^j}}{(M-m-l)!\mathrm{SNR}_0^{M-m-l}\widehat{\beta}\log_e 2}\right), \quad (21)$$

$\mathrm{VAR}(w_l/P_l)=v$is the same for $l=1,...,N_R$.To calculate SE, use $E_{v,h}[\mathrm{SE}(P/v,h)]$, where

$\mathrm{SE}(P/v,h)$is the SE of combining h and v. In prior discussions, the SE across a Rayleigh fading channel and AWGN was shown. $\mathrm{SE}(P/v)=E_h(\mathrm{SE}(P/v,h))$is the SE averaged over random channel realization h for fixed noise variance v. The average SE for different noise variances is:

$$E_{v,h}(\mathrm{SE}(P/v,h))=$$

$$E_v(\mathrm{SE}(P/v))=\sum_{m=0}^{\infty}\alpha_m\mathrm{SE}(P/v=\sigma_m^2), \quad (22)$$

IV. SIMULATIONS

This part confirms our system performance research with Monte Carlo simulations. We choose two sets of Z and X values to characterize a channel with near-Gaussian noise and one with extremely impulsive noise. 10000 channel realizations in MATLAB. Fig 2 illustrates SE Gaussian noise. Figure 3 through Figure 5demonstrate SE versus SNR for different IN settings and the near Gaussian situation when $Z=1$. Then we show alternative SE curves for Z, X,and $\widehat{\beta}$. Figures 6 to Figures 9illustrate the SE for *widehatbeta*.

Future research should explore the IN's implications in multiple MIMO scenarios, notably with diverse combining strategies. Post-detection and selection combining. Future study should include investigate IN under 5G MIMO approaches like NOMA.

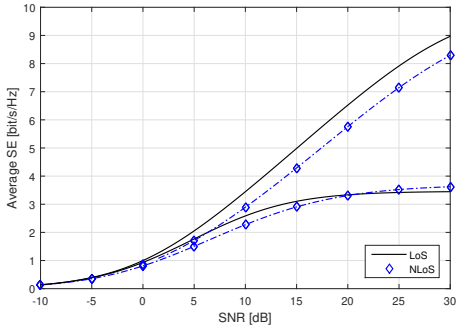

Fig. 2 SE versus $\mathrm{SNR_{dB}}$ for two values of interference power ratio $\widehat{\beta}=[10^{-3}\ 10^{-6}]$. Gaussian Noise Reference.

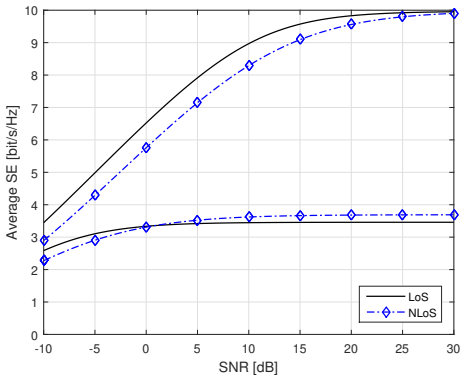

Fig. 3 SE versus $\mathrm{SNR_{dB}}$ for for two values of interference power ratio $\widehat{\beta}=[10^{-3}\ 10^{-6}]$. The Impulsive Index is $Z=10^{-4}$, the Gaussian to Non Gaussian power ratio is $X=0.1$.

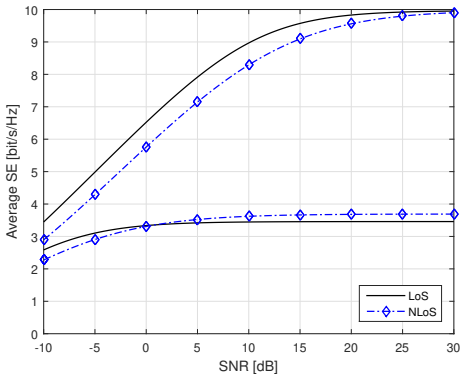

Fig. 4 SE versus $\mathrm{SNR_{dB}}$ for for two values of interference power ratio $\widehat{\beta}=[10^{-3}\ 10^{-6}]$. The Impulsive Index is $Z=10^{-2}$, the Gaussian to Non Gaussian power ratio is $X=0.1$.

V. CONCLUSIONS

In conclusion, the noise models discussed in this research study had no memory, that is the Middleton Class A. The suitable values for the Middleton Class A were then estimated in terms of the SE values for different model settings. It was also observed that when the impulsive noise values were set at large values then there was a similarity between the Middleton Class A

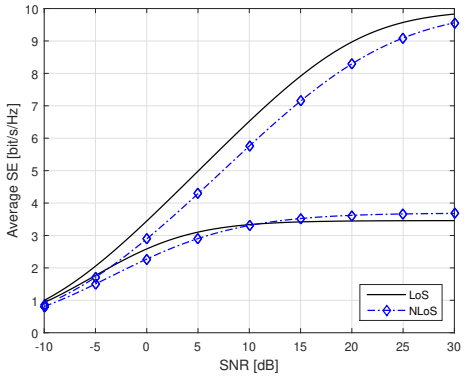

Fig. 5 SE versus $\mathrm{SNR_{dB}}$ for for two values of interference power ratio $\widehat{\beta} = [10^{-3}\ 10^{-6}]$. The Impulsive Index is $Z = 1$ (Near Gaussian scenario), the Gaussian to Non Gaussian power ratio is $X = 0.1$.

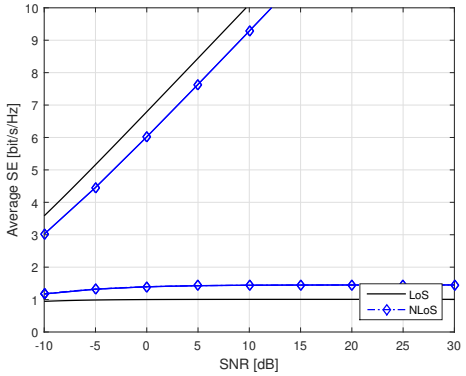

Fig. 6 SE versus $\mathrm{SNR_{dB}}$ for for two values of interference power ratio $\widehat{\beta} \approx [1\ 0]$. The Impulsive Index is $Z = 10^{-4}$, the Gaussian to Non Gaussian power ratio is $X = 0.1$.

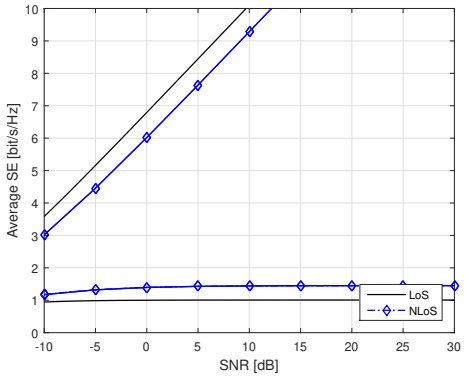

Fig. 7 SE versus $\mathrm{SNR_{dB}}$ for for two values of interference power ratio $\widehat{\beta} \approx [1\ 0]$. The Impulsive Index is $Z = 10^{-2}$, the Gaussian to Non Gaussian power ratio is $X = 0.1$.

and the Gaussian model. From the research study simulations, the SE mm Wave 5G systems execution efficiency under various models was illustrated. However, the main models illustrated were only two, that is the Gaussian model and the impulsive noise (IN) model. We conclude the conrtibutions as below points:

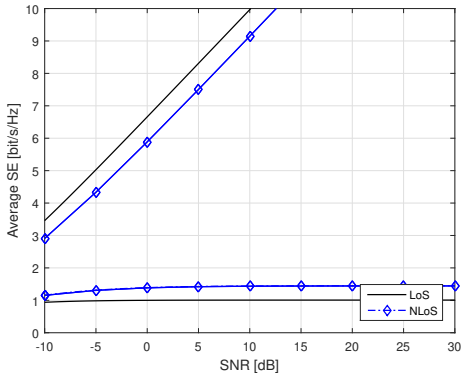

Fig. 8 SE versus $\mathrm{SNR_{dB}}$ for for two values of interference power ratio $\widehat{\beta} \approx [1\ 0]$. The Impulsive Index is $Z = 10^{-1}$, the Gaussian to Non Gaussian power ratio is $X = 0.1$.

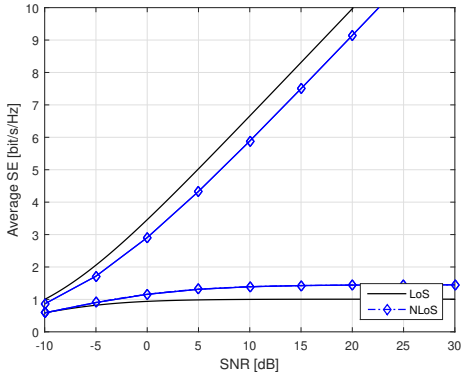

Fig. 9 SE versus $\mathrm{SNR_{dB}}$ for for two values of interference power ratio $\widehat{\beta} \approx [1\ 0]$. The Impulsive Index is $Z = 1$, the Gaussian to Non Gaussian power ratio is $X = 0.1$.

– The performance of SE mmWave 5G system under two noise models is shown. Mainly, the impulsive and Gaussian model.
– Fruitfull derivations were demonstrated and verified though MATLAB simulation.

VI. APPENDIX

Identity (1)

$$E\left\{log_2(1+\sum_{i=1}^{L}|b_i|^2)\right\} = \sum_{i=1}^{L}\frac{e^{\frac{1}{u_i}}E_1(1/u_i)}{log_e(2)\prod_{L=1,L\neq i}^{L}(1-u_L/u_i)}$$

,

REFERENCES

[1]. Kamili, A., Fatima, I., Hassan, M., Parah, S. A., Vijaya Kumar, V., and Ambati, L. S. , Embedding information reversibly in medical images for e-health , in Journal of Intelligent and Fuzzy Systems,(Preprint), 1-10. , (2020)

[2]. Ambati, L. S., El-Gayar, O., and Nawar, N. , In uence of The Digital Divide and Socio-Econpmic Factors on Prevalence Of Diabetes, in Issues in Information Sys- tems, 21(4), 103-113. , (2020)

[3]. El-Gayar, O. F., Ambati, L. S., and Nawar, N., Wearables, artificial intelligence, and the future of healthcare. In AI and Big Data's Potential for Disruptive Innovation , in IGI Global, (2020).(pp. 104-129).

[4]. Ambati, L. S., and El-Gayar, O. , Human Activity Recognition: A Comparison of Machine Learning Approaches. In AI and Big Data's Potential for Disruptive Innovation , in Journal of the Midwest Association for Information Systems, (2021).

[5]. I. P. Nasarre, T. Levanen, K. Pajukoski, A. Lehti, E. Tiirola and M. Valkama, Enhanced Uplink Coverage for 5G NR: Frequency-Domain Spectral Shaping With Spectral Extension, in IEEE Open Journal of the Com- munications Society, vol. 2, pp. 1188-1204, (2021), doi: 10.1109/OJCOMS.2021.3082688.

[6]. S. Niknam, B. Natarajan and R. Barazideh, Interference Analysis for Finite-Area 5G mmWave Networks Considering Blockage Effect, in IEEE Access, vol. 6, pp. 23470-23479, (2018), doi: 10.1109/ACCESS.2018.2829621.

[7]. F. A. Dicandia and S. Genovesi, Exploitation of Triangular Lattice Arrays for Improved Spectral Effi- ciency in Massive MIMO 5G Systems,in IEEE Ac- cess, vol. 9, pp. 17530-17543, (2021), doi: 10.1109/ACCESS.2021.3053091.

[8]. W. Hong et al., The Role of Millimeter-Wave Technologies in 5G/6G Wireless Communications, in IEEE Jour- nal of Microwaves, vol. 1, no. 1, pp. 101-122, Jan. (2021), doi: 10.1109/JMW.2020.3035541.

[9]. J. P. Santacruz, S. Rommel, U. Johannsen, A. Jurado-Navas and I. T. Monroy, Analysis and Compensation of Phase Noise in Mm-Wave OFDM ARoF Systems for Beyond 5G, in Journal of Lightwave Technology, vol. 39, no. 6, pp. 1602-1610, 15 March15, (2021), doi: 10.1109/JLT.2020.3041041.

[10]. M. S. Alam, B. Selim, I. Ahmed, G. Kaddoum and H. Yanikomeroglu, Bursty Impulsive Noise Mitigation in NOMA: A MAP Receiver-Based Approach, in IEEE Communications Letters, vol. 25, no. 9, pp. 2790-2794, Sept. (2021), doi: 10.1109/LCOMM.2021.3089725.

[11]. J. Wang et al., Spectral Efficiency Improvement With 5G Technologies: Results From Field Tests, in IEEE Journal on Selected Areas in Communica- tions, vol. 35, no. 8, pp. 1867-1875, Aug. (2017), doi: 10.1109/JSAC.2017.2713498.

[12]. P. Patcharamaneepakorn et al., Spectral, Energy, and Economic Efficiency of 5G Multicell Massive MIMO Systems With Generalized Spatial Modulation, in IEEE Transactions on Vehicular Technology, vol. 65, no. 12, pp. 9715-9731, Dec. (2016), doi: 10.1109/TVT.2016.2526628.

[13]. M. Mulla, A. H. Ulusoy, A. Rizaner and H. Amca, Barzilai-Borwein Gradient Algorithm Based Alternat- ing Minimization for Single User Millimeter Wave Systems, in IEEE Wireless Communications Let- ters, vol. 9, no. 4, pp. 508-512, April (2020), doi: 10.1109/LWC.2019.2960691.

[14]. Abuhilal, Hasan, Aykut Hocanin, and Huseyin Bilgekul. Successive interference cancelation for a CDMA system with diversity reception in non-Gaussian noise. Interna- tional Journal of Communication Systems 26.7 (2013): 875-887.

[15]. Mulla, M., Rizaner, A. and Ulusoy, A.H. Fuzzy Logic Based Decoder for Single-User Millimeter Wave Sys- tems Under Impulsive Noise. Wireless Pers Commun, Springer (2021).

[16]. Abu Hilal, H. Error Rate Analysis of ZF and MMSE Decoders for Massive Multi Cell MIMO Systems in Impulsive Noise Channels. Int J Wireless Inf Networks, Springer 26, 80-89 (2019).

[17]. Abu Hilal, H. Performance of ZF and MMSE decoders for massive multi-cell MIMO systems in impulsive and Lapla- cian noise channels. SIViP, Springer 14, 49-56 (2020).

[18]. H. A. Hilal and T. A. Hilal, Impact of impulsive noise on 4G OFDM and SCFDMA systems, 2017 IEEE International Symposium on Signal Processing and Information Technology (ISSPIT), 2017, pp. 180-185, doi: 10.1109/ISSPIT.2017.8388638.

[19]. Hasan Abu Hilal, Neural networks applications for CDMA systems in non-Gaussian multi-path channels, AEU - International Journal of Electronics and Com- munications, Elsevier, Volume 73,

[20]. Ahmad, M.S., Kukrer, O. and Hocanin, A. Robust Recursive Inverse Adaptive Algorithm in Impulsive Noise. Circuits Syst Signal Process 31, 703-710 (2012).

[21]. OM Shekoni, AN Hasan, T Shongwe, Applications of ar- tificial intelligence in powerline communications in terms of noise detection and reduction: a review, Australian Journal of Electrical and Electronics Engineering 15 (1- 2), 29-37

[22]. Mohammad Sirajuddin, Ch. Rupa, Celestine Iwendi, and Cresantus Biamba TBSMR: A Trust-Based Secure Multipath Routing Protocol for Enhancing the QoS of the Mobile Ad Hoc Network, Security and Communication Networks, Hindawi. DOI: 5521713. (2021)

[23]. J. H. Anajemba, T. Yue, C. Iwendi, M. Alenezi and M. Mittal, "Optimal Cooperative Offloading Scheme for Energy Efficient Multi-Access Edge Computation," in IEEE Access, vol. 8, pp. 53931-53941, 2020, doi: 10.1109/ACCESS.2020.2980196.

[24]. J. H. Anajemba, T. Yue, C. Iwendi, P. Chatterjee, D. Ngabo and W. S. Alnumay, "A Secure Multiuser Privacy Technique for Wireless IoT Networks Using Stochastic Privacy Optimization," in IEEE Internet of Things Jour- nal, vol. 9, no. 4, pp. 2566-2577, 15 Feb.15, 2022, doi: 10.1109/JIOT.2021.3050755.
[25]. D. Middleton. Aug. 1977. Statistical-physical models of electromagnetic interference, IEEE Trans. Electromag. Compat., vol. EC-19, pp. 106-127.
[26]. Bjornson, Jakob Hoydis and Luca Sanguinetti , Massive MIMO Networks: Spectral, Energy, and Hardware Ef- ficiency, Foundations and Trends in Signal Processing: Vol. 11, No. 3-4,pp. 154-655. DOI: 10.1561/2000000093. (2017)